INTERNATIONAL JOURNAL FOR NUMERICAL METHODS IN ENGINEERING
Int. J. Numer. Meth. Engng 2004; **59**:1657–1678 (DOI: 10.1002/nme.935)

Which are the important modes of a subsystem?

Dan Givoli[1,*,†,‡], Paul E. Barbone[2] and Igor Patlashenko[3]

[1]*Department of Aerospace Engineering and Asher Space Research Center, Technion, Haifa 32000, Israel*
[2]*Department of Aerospace and Mechanical Engineering, Boston University, 110 Cummington Street, Boston, MA 02215, U.S.A.*
[3]*Performance Group, EMC Corporation, 171 South Street, Hopkinton, MA 01748-9103, U.S.A.*

SUMMARY

A linearly behaving vibrational substructure (or more generally a linear dynamic subsystem) attached to a main structure (or a main dynamic system) is considered. After discretization, the substructure is represented by a finite, typically large, number of degrees of freedom, N_s and hence also by N_s eigenmodes. In order to reduce the computational effort, it is common to apply 'modal reduction' to the subsystem such that only N_r modes out of the total number of N_s modes are retained, where $N_r \ll N_s$. The following question then arises: '*Which* N_r modes should be retained?' In structural dynamics, it is traditional to retain those modes associated with the lowest frequencies. In this paper, the question is answered by solving an appropriate optimization problem. The most important modes of the subsystem are shown to be those whose coupling matrices, which are defined in a particular way, have the highest norm. This leads to a simple and effective algorithm for optimal modal reduction. The new criterion for 'modal importance' is explained both mathematically and physically, and is demonstrated by numerical examples. Copyright © 2004 John Wiley & Sons, Ltd.

KEY WORDS: subsystem; dynamic system; model reduction; modal reduction; Dirichlet-to-Neumann; vibration; finite elements

1. INTRODUCTION

One of the fundamental problems of linear system theory is the approximation of complex systems by simpler ones. In the context of structural dynamics, the goal is to approximate a given discrete model of a structure by another model which involves a much smaller number of degrees of freedom. Such a reduction is very important in cases where the computational

*Correspondence to: Don Givoli, Department of Aerospace Engineering and Asher Space Research Center, Technion, Haifa 32000, Israel.
†E-mail: givolid@aerodyne.technion.ac.il
‡Part of this work was done while on leave at the Department of Mathematics, Naval Postgraduate School, Monterey, CA, U.S.A.

Contract/grant sponsor: U.S.–Israel Binational Science Foundation (BSF) Fund; contract/grant number: 97-00120
Contract/grant sponsor: The fund for the Promotion of Research at the Technion

Received 9 December 2002
Revised 18 June 2003
Accepted 9 July 2003

effort associated with the direct analysis of the given system is prohibitive. There is a very large volume of literature on the subject, often called 'model order reduction;' see, e.g. the review papers [1–5]. Some of this work is related to robust control, where there is a need for the repetitive real-time solution of large structural dynamic problems [6].

One major way to simplify models is via *modal reduction*. The original linear system is first decomposed into its eigenmodes. Then a small number of these eigenmodes is retained to represent the system, whereas all the other modes are discarded. The following question then arises: '*Which* of the modes should be retained?' In structural dynamics, it is traditional to retain those modes associated with the *lowest frequencies* [7]. In control theory, a common procedure is the balanced realization method proposed by Moore [8], where a special mode truncation is used to obtain a reduced system with equal amount of controllability and observability. Both these approaches are simple and easy to code, but they are not based on any optimality criterion. Hence, although in many cases they produce very good approximations, they are not guaranteed to do so.

There are also model reduction methods which are not based on modal truncation. One very simple procedure, used mainly in aeroelasticity, is Guyan reduction which is an approximate dynamical analogue of static condensation [9]. The next level of complexity in structural dynamic condensation is 'component mode synthesis'. In this case, the response of the subsystem is projected via a Ritz reduction procedure onto a collection of vectors which are described as rigid body 'modes', dynamic 'modes' and constraint 'modes' [10]. In the robust controls literature, we can find reduction schemes on the other end of the spectrum of complexity. The optimal projection method of Hyland and Bernstein [11], for example, is an optimization method which guarantees a minimum reduction error using a quadratic error criterion. Both the theoretical considerations and the practical implementation of this method are much more complicated than those of balanced realization, component mode synthesis, or Guyan reduction.

These methods are applied, in most cases, to an entire dynamic system with given boundary conditions, whose reduction is desired. In this paper, we consider a slightly different perspective. We consider a linear subsystem 'attached' to a main system. In the context of structural dynamics, such a subsystem may represent a piece of equipment, antenna, etc., connected to the main structure. On the other hand, if an engineer is interested in the dynamics of different antenna designs, the 'subsystem' may be most of the structure, while the antenna may be treated as the 'main' structure. We wish to reduce the subsystem alone, without modifying the main system. When doing this, we are not interested in the accurate representation of the dynamics of the subsystem itself, but in accurately representing the effect this subsystem has on the dynamic behaviour of the main structure.

Recently, we have considered the *exact* representation of a dynamic linear substructure using a reduced number of degrees of freedom [12]. This is achieved by transforming the equations of motion of the substructure to a system of integro-differential equations on the interface between the substructure and the main structure, which are appended to the differential equations of motion of the main structure. In Reference [12] several time-integration schemes for the solution of the resulting equations have been introduced and analysed.

In this paper, we concentrate on the modal reduction of a linear subsystem with no damping. We ask a question similar to the one mentioned above: In the reduction process, *which of the subsystem's modes should be retained*? In contrast to the low-frequency rule dominating structural dynamics, we shall obtain a new criterion for 'modal importance'. We shall show that the most important modes of the subsystem are those whose coupling matrices, to be

defined in a particular way, have the highest norm. This will lead to a simple and effective algorithm for optimal modal reduction. We shall explain the new criterion both mathematically and physically and shall demonstrate it via numerical examples.

In Reference [13] we have looked into a similar problem in a simplified setting. In particular, we assumed in Reference [13] that the mass matrix of the original subsystem is partially *lumped*. Here we shall remove this limiting assumption, with the price of making the formulation slightly more complicated. In addition, we shall provide a physical explanation and some illustrative examples to our 'modal importance' criterion which were lacking in Reference [13]. We shall also present the whole procedure in a slightly different way than we have done in Reference [13], by using modal truncation from the outset and omitting the assumption of long simulation times. We note that in Reference [13], we show that of all Ritz reduction procedures, modal truncation is in a certain sense optimal.

The outline of the rest of the paper is as follows. In Section 2, we provide the detailed statement of the reduction problem under consideration. The formulation of this problem is based on the notion of the Dirichlet-to-Neumann (DtN) map, a concept whose relevance to the present problem we explain. In Section 3, we derive the appropriate DtN map, and define the coupling matrix of a mode. This matrix is related to the amount of coupling existing between the subsystem and the main system. In Section 4, we use these concepts to derive the solution to the reduction problem. This involves the formulation of a criterion for choosing the subsystem's most important modes. We then present a modal reduction algorithm based on this criterion. In Section 5, we provide the physical interpretation of the 'modal importance criterion' and illustrate it via examples. We present some numerical results in Section 6, which are compared to those obtained by standard modal reduction (the latter being based on retaining the lowest-frequency modes). We conclude with some remarks in Section 7.

2. STATEMENT OF THE PROBLEM

We consider the vibrational motion of a structure consisting of a main part and an attached part, which interact with each other through an interface. We assume that the structure behaves linearly and that no damping is involved. More generally, one may have a main structure attached to several substructures. However, as long as the different substructures do not interact directly with each other but only through the main structure, the methodology proposed here can be applied to each substructure separately.

After spatial discretization, say by finite elements, the structural model becomes a linear dynamic system consisting of a main part indicated by 'm', and an additional subsystem indicated by 's'. The discrete interface separating 'm' and 's' is indicated by 'b'. We denote the number of degrees of freedom inside 'm', on 'b' and inside 's' by N_{m}, N_{b} and N_{s}, respectively. Thus, the total number of degrees of freedom in the entire system is $N = N_{\mathrm{m}} + N_{\mathrm{b}} + N_{\mathrm{s}}$. The set-up is illustrated in the upper part of Figure 1.

We remark that although the description above involves structures, the problem discussed here is quite general and can involve various other types of linear dynamical systems as well.

The global discrete system is written in the standard form

$$\mathbf{M}\ddot{\mathbf{u}}(t) + \mathbf{K}\mathbf{u}(t) = \mathbf{F}(t) \tag{1}$$

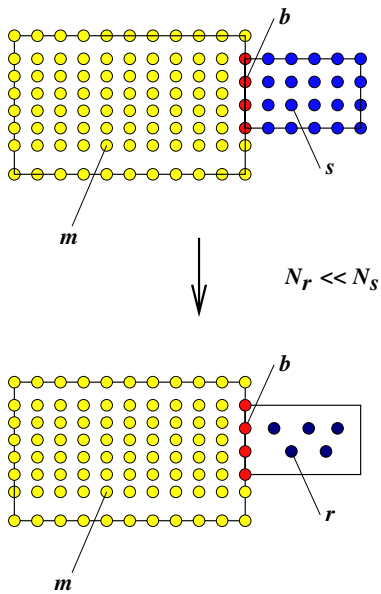

Figure 1. Set-up for the subsystem reduction problem.

Here t is time, and a superposed dot indicates time differentiation. In the terminology of structural dynamics, $\mathbf{M}$ is the global mass matrix, $\mathbf{K}$ is the global stiffness matrix, $\mathbf{F}$ is the global load vector and $\mathbf{u}(t)$ is the unknown vector of displacements. $\mathbf{M}$ and $\mathbf{K}$ are assumed to be constant real symmetric matrices; $\mathbf{M}$ is positive definite while $\mathbf{K}$ is positive semi-definite. All the above-mentioned arrays are of dimension N. Initial conditions for $\mathbf{u}(t)$ at time $t = 0$ are given as well:

$$\mathbf{u}(0) = \mathbf{u}_0, \quad \dot{\mathbf{u}}(0) = \mathbf{v}_0 \tag{2}$$

The vector of unknowns $\mathbf{u}$ is partitioned into three subvectors, i.e. $\mathbf{u}^{\mathrm{T}} = \{\mathbf{u}_{\mathrm{m}}\ \mathbf{u}_{\mathrm{b}}\ \mathbf{u}_{\mathrm{s}}\}$, representing the degrees of freedom inside the main system, on the interface and inside the subsystem, respectively. Here and elsewhere, the superscript T denotes vector or matrix transposition. Thus, (1) can be written in a partitioned form as

$$\begin{bmatrix} \mathbf{M}_{\mathrm{mm}} & \mathbf{M}_{\mathrm{mb}} & \mathbf{0} \\ \mathbf{M}_{\mathrm{bm}} & \mathbf{M}_{\mathrm{bb}} & \mathbf{M}_{\mathrm{bs}} \\ \mathbf{0} & \mathbf{M}_{\mathrm{sb}} & \mathbf{M}_{\mathrm{ss}} \end{bmatrix} \begin{Bmatrix} \ddot{\mathbf{u}}_{\mathrm{m}} \\ \ddot{\mathbf{u}}_{\mathrm{b}} \\ \ddot{\mathbf{u}}_{\mathrm{s}} \end{Bmatrix} + \begin{bmatrix} \mathbf{K}_{\mathrm{mm}} & \mathbf{K}_{\mathrm{mb}} & \mathbf{0} \\ \mathbf{K}_{\mathrm{bm}} & \mathbf{K}_{\mathrm{bb}} & \mathbf{K}_{\mathrm{bs}} \\ \mathbf{0} & \mathbf{K}_{\mathrm{sb}} & \mathbf{K}_{\mathrm{ss}} \end{bmatrix} \begin{Bmatrix} \mathbf{u}_{\mathrm{m}} \\ \mathbf{u}_{\mathrm{b}} \\ \mathbf{u}_{\mathrm{s}} \end{Bmatrix} = \begin{Bmatrix} \mathbf{F}_{\mathrm{m}} \\ \mathbf{0} \\ \mathbf{0} \end{Bmatrix} \tag{3}$$

The zero blocks in the mass and stiffness matrices appear due to the fact that the subsystem 's' and the main system 'm' are coupled only through the interface degrees of freedom 'b'. Owing to the symmetry of $\mathbf{K}$ and $\mathbf{M}$, all the diagonal block matrices in (3) are symmetric, while the off-diagonal rectangular blocks are equal to the transpose of their reflections, namely $\mathbf{M}_{\mathrm{mb}} = \mathbf{M}_{\mathrm{bm}}^{\mathrm{T}}$, etc. The dimensions of the various arrays are obvious, e.g. $\mathbf{M}_{\mathrm{mb}}$ is an $N_{\mathrm{m}} \times N_{\mathrm{b}}$

matrix. We assume that all the external loading is applied to the main system, and thus the subsystem and the interface are unloaded externally. This explains the two zero subvectors in the load vector $\mathbf{F}$ in (3). We further assume that all non-zero initial conditions apply to the main system only, namely

$$\mathbf{u}_{\mathrm{m}}(0) = \mathbf{u}_{\mathrm{m}0}, \quad \dot{\mathbf{u}}_{\mathrm{m}}(0) = \mathbf{v}_{\mathrm{m}0}, \quad \mathbf{u}_{\mathrm{b}}(0) = \mathbf{0}, \quad \dot{\mathbf{u}}_{\mathrm{b}}(0) = \mathbf{0}, \quad \mathbf{u}_{\mathrm{s}}(0) = \mathbf{0}, \quad \dot{\mathbf{u}}_{\mathrm{s}}(0) = \mathbf{0} \tag{4}$$

Assuming the number of degrees of freedom N_{s} of the given subsystem is too large for practical computation, we wish to replace the subsystem 's' by a new subsystem 'r' (see Figure 1) with N_{r} degrees of freedom and with the following properties:

1. The subsystem 'r' should be *computationally efficient*, namely it should have a much smaller number of degrees of freedom than the original 's': $N_{\mathrm{r}} \ll N_{\mathrm{s}}$.
2. The subsystem 'r' should be *modular*, namely the properties of 'r' should be determined entirely in terms of the properties of 's' (i.e. independent of the properties of 'm').
3. The subsystem 'r' should be a *good approximation* of the original 's', in that the replacement of 's' by 'r' should have the smallest possible effect on the dynamics of the main system 'm'.

The need for properties 1 and 3 is obvious. Property 2 is required to allow a subsystem model to be used with different main systems. For example, if the subsystem is an aeroengine, an engineer may be interested in determining the effects of the aeroengine on the dynamics of wings of different geometries. Thus, it is important to make the reduction based on just the properties of the subsystem. This criterion is distinct from typical reduction procedures found in the controls community [6].

We make a few remarks regarding the properties above:

- It is important to note that the *computational cost associated with the model reduction is not of a major concern* here. The reason is that in most cases the reduction algorithm is employed one time in order to produce a reduced model which is then used many times with various inputs (external loads and initial conditions). Thus, in many cases one is willing to invest a lot of effort in reducing a given system. This is especially so in substructuring and in real-time control applications, and it is the former that motivates the authors' current interest. In fact, some reduction methods involve the one-time solution of the full original system for a specific input (e.g. a Dirac-delta input), or the full spectral decomposition of the original system. In the latter case, approximate, relatively fast, methods of spectral decomposition may be used to reduce the computational cost in the reduction process if one is willing to compromise the modal accuracy.
- The main concern here is the dynamical behaviour of the main system 'm'; it is assumed that *the dynamics of the subsystem* 's' *itself is not of interest*. Yet, the subsystem must be represented sufficiently well since *the effect that it has on the main system* is very important in determining the dynamical response of the latter. If a poor reduced model is used for the given subsystem, it may produce a large error in the dynamics of the main system as well.
- If the discretization that leads to the linear system is performed using the standard finite element method, then the degrees of freedom of 'm', 'b' and 's' are nodal values of the solution (nodal displacements in the case of a vibrating structure). However, after reduction, *the degrees of freedom of the new subsystem* 'r' *should not necessarily be*

nodal solutions. In fact, they do not have to possess any physical meaning at all, as long as they accurately preserve the effect the subsystem has on the main system.

Mathematically, the linear system (3) is replaced with the smaller system

$$\begin{bmatrix} \mathbf{M}_{\mathrm{mm}} & \mathbf{M}_{\mathrm{mb}} & \mathbf{0} \\ \mathbf{M}_{\mathrm{bm}} & \mathbf{m}_{\mathrm{bb}} & \mathbf{m}_{\mathrm{br}} \\ \mathbf{0} & \mathbf{m}_{\mathrm{rb}} & \mathbf{m}_{\mathrm{rr}} \end{bmatrix} \begin{Bmatrix} \ddot{\mathbf{u}}_{\mathrm{m}} \\ \ddot{\mathbf{u}}_{\mathrm{b}} \\ \ddot{\mathbf{u}}_{\mathrm{r}} \end{Bmatrix} + \begin{bmatrix} \mathbf{K}_{\mathrm{mm}} & \mathbf{K}_{\mathrm{mb}} & \mathbf{0} \\ \mathbf{K}_{\mathrm{bm}} & \mathbf{k}_{\mathrm{bb}} & \mathbf{k}_{\mathrm{br}} \\ \mathbf{0} & \mathbf{k}_{\mathrm{rb}} & \mathbf{k}_{\mathrm{rr}} \end{bmatrix} \begin{Bmatrix} \mathbf{u}_{\mathrm{m}} \\ \mathbf{u}_{\mathrm{b}} \\ \mathbf{u}_{\mathrm{r}} \end{Bmatrix} = \begin{Bmatrix} \mathbf{F}_{\mathrm{m}} \\ \mathbf{0} \\ \mathbf{0} \end{Bmatrix} \tag{5}$$

Here $\mathbf{u}_{\mathrm{r}}(t)$ is the N_{r}-dimensional unknown vector associated with the reduced subsystem. The two linear systems (3) and (5) differ in that $\mathbf{u}_{\mathrm{s}}$ is replaced by the shorter vector $\mathbf{u}_{\mathrm{r}}$, and the block matrices $\mathbf{M}_{\mathrm{bb}}$, $\mathbf{M}_{\mathrm{bs}} = \mathbf{M}_{\mathrm{sb}}^{\mathrm{T}}$, $\mathbf{M}_{\mathrm{ss}}$, $\mathbf{K}_{\mathrm{bb}}$, $\mathbf{K}_{\mathrm{bs}} = \mathbf{K}_{\mathrm{sb}}^{\mathrm{T}}$ and $\mathbf{K}_{\mathrm{ss}}$ are replaced by $\mathbf{m}_{\mathrm{bb}}$, $\mathbf{m}_{\mathrm{br}} = \mathbf{m}_{\mathrm{rb}}^{\mathrm{T}}$, $\mathbf{m}_{\mathrm{rr}}$, $\mathbf{k}_{\mathrm{bb}}$, $\mathbf{k}_{\mathrm{br}} = \mathbf{k}_{\mathrm{rb}}^{\mathrm{T}}$ and $\mathbf{k}_{\mathrm{rr}}$, respectively.

We remark that at first sight the necessity to replace $\mathbf{M}_{\mathrm{bb}}$ and $\mathbf{K}_{\mathrm{bb}}$ by other matrices $\mathbf{m}_{\mathrm{bb}}$ and $\mathbf{k}_{\mathrm{bb}}$ is not obvious, since the new matrices have exactly the same dimensions as the old ones ($N_{\mathrm{b}} \times N_{\mathrm{b}}$); however, it turns out that performing such a modification is beneficial in that it leads to a smaller reduction error. This has been shown in a simpler setting in Reference [13], and will become clear in this paper too. Furthermore, it may seem like such a replacement violates requirement 2, above. We note, however, that $\mathbf{M}_{\mathrm{bb}}$ and $\mathbf{K}_{\mathrm{bb}}$ have contributions from both the main system and the subsystem, e.g.

$$\mathbf{K}_{\mathrm{bb}} = \mathbf{K}_{\mathrm{bb}}^{(\mathrm{m})} + \mathbf{K}_{\mathrm{bb}}^{(\mathrm{s})} \tag{6}$$

Requirement 2 allows modifying $\mathbf{M}^{(\mathrm{s})}{}_{\mathrm{bb}}$ and $\mathbf{K}^{(\mathrm{s})}{}_{\mathrm{bb}}$, which manifests itself more broadly as a change to $\mathbf{M}_{\mathrm{bb}}$ and $\mathbf{K}_{\mathrm{bb}}$.

The initial conditions (see (4)) dictate that

$$\mathbf{u}_{\mathrm{r}}(0) = \mathbf{0}, \quad \dot{\mathbf{u}}_{\mathrm{r}}(0) = \mathbf{0} \tag{7}$$

The problem to be solved is thus: Find the six matrices $\mathbf{m}_{\mathrm{bb}}$, $\mathbf{m}_{\mathrm{br}} = \mathbf{m}_{\mathrm{rb}}^{\mathrm{T}}$, $\mathbf{m}_{\mathrm{rr}}$, $\mathbf{k}_{\mathrm{bb}}$, $\mathbf{k}_{\mathrm{br}} = \mathbf{k}_{\mathrm{rb}}^{\mathrm{T}}$ and $\mathbf{k}_{\mathrm{rr}}$ such that for arbitrary external load and initial conditions the behaviour of the main system 'm' in the reduced system (5) be as 'similar' as possible to that of 'm' in the original system (3). Of course, there are various ways to define the norm in which this similarity is measured. We choose a specific norm, based on the *DtN map*.

In the context of discrete structural models, the DtN map is the operator relating the displacement and force on a certain boundary interface. In shell theory, this operator is sometimes called the 'interface stiffness' or 'edge stiffness' [14]. More generally, it is the operator relating the primary field and its 'flux' on an interface. This operator is a good measure of the effect that a part of the system lying on one side of the interface has on the other part. The use of the DtN map in computational schemes was originally developed by Keller and Givoli [15, 16] for the solution of boundary value problems in unbounded domains. Later, the concept was also used for the solution of problems with geometrical singularities [17]. Much more recently, the DtN method was applied to linear dynamical systems by Barbone *et al.* [18–20]. See also the review paper [21].

Relating to Figure 1, the DtN map associated with the interface 'b' will be considered. The proposed viewpoint is as follows. Since the subsystem 's' interacts with the main system 'm' only through the interface 'b', the effect that 's' has on 'm' is characterized by the DtN map Γ

on 'b'. This is true also for the reduced system, namely the effect that the reduced subsystem 'r' has on 'm' is characterized by $\tilde{\Gamma}$, which is the DtN map on 'b' associated with the reduced subsystem. Now, consider the 'distance' between Γ and $\tilde{\Gamma}$ in some appropriate norm. We shall find the reduced subsystem 'r' for which this 'distance' is minimized.

We now put this idea in mathematical terms. Thinking of $\mathbf{u}$ as a vector of displacements, we first find the forces applied to the interface by the subsystem (and by the interface itself). From the middle set of Equations in (3) (for the original system) and in (5) (for the reduced system) we have

$$\mathbf{M}_{\mathrm{bm}}\ddot{\mathbf{u}}_{\mathrm{m}} + \mathbf{K}_{\mathrm{bm}}\mathbf{u}_{\mathrm{m}} = -\mathbf{M}_{\mathrm{bb}}\ddot{\mathbf{u}}_{\mathrm{b}} - \mathbf{M}_{\mathrm{bs}}\ddot{\mathbf{u}}_{\mathrm{s}} - \mathbf{K}_{\mathrm{bb}}\mathbf{u}_{\mathrm{b}} - \mathbf{K}_{\mathrm{bs}}\mathbf{u}_{\mathrm{s}} \tag{8}$$

$$\mathbf{M}_{\mathrm{bm}}\ddot{\tilde{\mathbf{u}}}_{\mathrm{m}} + \mathbf{K}_{\mathrm{bm}}\tilde{\mathbf{u}}_{\mathrm{m}} = -\mathbf{m}_{\mathrm{bb}}\ddot{\tilde{\mathbf{u}}}_{\mathrm{b}} - \mathbf{m}_{\mathrm{br}}\ddot{\mathbf{u}}_{\mathrm{r}} - \mathbf{k}_{\mathrm{bb}}\tilde{\mathbf{u}}_{\mathrm{b}} - \mathbf{k}_{\mathrm{br}}\mathbf{u}_{\mathrm{r}} \tag{9}$$

The notation $\tilde{\mathbf{u}}_{\mathrm{m}}$ and $\tilde{\mathbf{u}}_{\mathrm{b}}$ has been used here for the independent variables of the reduced system. The right-hand sides of (8) and (9) give us expressions for the interface forces:

$$\mathbf{f}_{\mathrm{b}}(t) = \Gamma\mathbf{u}(t) \equiv -\mathbf{M}_{\mathrm{bb}}\ddot{\mathbf{u}}_{\mathrm{b}} - \mathbf{M}_{\mathrm{bs}}\ddot{\mathbf{u}}_{\mathrm{s}} - \mathbf{K}_{\mathrm{bb}}\mathbf{u}_{\mathrm{b}} - \mathbf{K}_{\mathrm{bs}}\mathbf{u}_{\mathrm{s}} \tag{10}$$

$$\tilde{\mathbf{f}}_{\mathrm{b}}(t) = \tilde{\Gamma}\mathbf{u}(t) \equiv -\mathbf{m}_{\mathrm{bb}}\ddot{\mathbf{u}}_{\mathrm{b}} - \mathbf{m}_{\mathrm{br}}\ddot{\mathbf{u}}_{\mathrm{r}} - \mathbf{k}_{\mathrm{bb}}\mathbf{u}_{\mathrm{b}} - \mathbf{k}_{\mathrm{br}}\mathbf{u}_{\mathrm{r}} \tag{11}$$

Note that these quantities are 'forces' in the D'Alembert sense, namely they include inertial loads. Also, note that we have omitted the ˜ from the interface displacement in the reduced system, since we are interested in comparing the forces produced by the original and by the reduced subsystems for the *same* given interface displacement. Finally, note that both force vectors $\mathbf{f}_{\mathrm{b}}$ and $\tilde{\mathbf{f}}_{\mathrm{b}}$ are of dimension N_{b}.

We consider now the distance between these two vectors. More precisely, we define

$$\Pi \equiv \|\mathbf{f}_{\mathrm{b}} - \tilde{\mathbf{f}}_{\mathrm{b}}\|_T = \|\Gamma\mathbf{u} - \tilde{\Gamma}\mathbf{u}\|_T \tag{12}$$

where $\|\cdot\|_T$ is the norm defined by

$$\|\mathbf{f}\|_T = \frac{1}{T}\int_0^T |\mathbf{f}(t)|^2\,\mathrm{d}t \tag{13}$$

In (13), T is a given time value which represents the time span of interest ('simulation time'). Now our goal is to find the matrices comprising the reduced system such that Π is minimized.

In the next two sections, we solve this minimization problem within the framework of modal analysis, and show that its solution amounts to a certain criterion for choosing the most important modes of the subsystem.

3. THE DIRICHLET-TO-NEUMANN (DtN) MAP

The quantity Π defined in the previous section measures the distance between the DtN maps Γ and $\tilde{\Gamma}$ (where $\Gamma\mathbf{u} = \mathbf{f}_{\mathrm{b}}$ and $\tilde{\Gamma}\mathbf{u} = \tilde{\mathbf{f}}_{\mathrm{b}}$) on the interface 'b'. In this section, we shall derive expressions for these DtN maps.

We start with the original subsystem 's'. We consider the generalized eigenvalue problem associated with it:

$$\mathbf{K}_{\mathrm{ss}}\boldsymbol{\phi} = \omega^2\mathbf{M}_{\mathrm{ss}}\boldsymbol{\phi} \tag{14}$$

We assume that the matrices $\mathbf{M}_{\mathrm{ss}}$ and $\mathbf{K}_{\mathrm{ss}}$ are symmetric and positive definite.

The solution of (14) yields N_{s} eigenfrequencies ω_n and N_{s} corresponding eigenvectors $\boldsymbol{\phi}_n$. The eigenvectors are orthogonal with respect to the mass matrix and are normalized so that

$$\boldsymbol{\phi}_{\mathrm{m}}^{\mathrm{T}}\mathbf{M}_{\mathrm{ss}}\boldsymbol{\phi}_n = \delta_{\mathrm{m}n} \tag{15}$$

where $\delta_{\mathrm{m}n}$ is the Kronecker delta. From (14) and (15) we also have

$$\boldsymbol{\phi}_{\mathrm{m}}^{\mathrm{T}}\mathbf{K}_{\mathrm{ss}}\boldsymbol{\phi}_n = \delta_{\mathrm{m}n}\omega_n^2 \tag{16}$$

The last two orthogonality statements can also be written as

$$\boldsymbol{\Phi}^{\mathrm{T}}\mathbf{M}_{\mathrm{ss}}\boldsymbol{\Phi} = \mathbf{I} \tag{17}$$

$$\boldsymbol{\Phi}^{\mathrm{T}}\mathbf{K}_{\mathrm{ss}}\boldsymbol{\Phi} = \boldsymbol{\Omega}^2 \tag{18}$$

where $\boldsymbol{\Phi}$ is the $N_{\mathrm{s}} \times N_{\mathrm{s}}$ matrix whose columns are the eigenvectors $\boldsymbol{\phi}_n$, $\mathbf{I}$ is the $N_{\mathrm{s}} \times N_{\mathrm{s}}$ identity, and $\boldsymbol{\Omega}^2$ is the $N_{\mathrm{s}} \times N_{\mathrm{s}}$ diagonal matrix whose diagonal entries are the squared frequencies ω_n^2.

Now, the third set of equations in (3) describes the dynamics of 's':

$$\mathbf{M}_{\mathrm{ss}}\ddot{\mathbf{u}}_{\mathrm{s}} + \mathbf{K}_{\mathrm{ss}}\mathbf{u}_{\mathrm{s}} = -\mathbf{M}_{\mathrm{sb}}\ddot{\mathbf{u}}_{\mathrm{b}} - \mathbf{K}_{\mathrm{sb}}\mathbf{u}_{\mathrm{b}} \tag{19}$$

We diagonalize this equation by making use of the solutions to the generalized eigenvalue problem (14). To this end, we expand $\mathbf{u}_{\mathrm{s}}$ in the eigenvectors $\boldsymbol{\phi}_n$, i.e.

$$\mathbf{u}_{\mathrm{s}}(t) = \sum_{n=1}^{N_{\mathrm{s}}} \boldsymbol{\phi}_n Y_n(t) \equiv \boldsymbol{\Phi}\mathbf{Y}(t) \tag{20}$$

where the $Y_n(t)$ are scalar functions of time. We substitute (20) in (19) and multiply the equation on the left by $\boldsymbol{\Phi}^{\mathrm{T}}$. Then by using the orthogonality properties (17) and (18) we obtain

$$\ddot{\mathbf{Y}} + \boldsymbol{\Omega}^2\mathbf{Y} = -\boldsymbol{\Phi}^{\mathrm{T}}\mathbf{M}_{\mathrm{sb}}\ddot{\mathbf{u}}_{\mathrm{b}} - \boldsymbol{\Phi}^{\mathrm{T}}\mathbf{K}_{\mathrm{sb}}\mathbf{u}_{\mathrm{b}} \tag{21}$$

In component form this equation becomes

$$\ddot{Y}_n(t) + \omega_n^2 Y_n(t) = -\boldsymbol{\phi}_n^{\mathrm{T}}\mathbf{M}_{\mathrm{sb}}\ddot{\mathbf{u}}_{\mathrm{b}}(t) - \boldsymbol{\phi}_n^{\mathrm{T}}\mathbf{K}_{\mathrm{sb}}\mathbf{u}_{\mathrm{b}}(t) \equiv \dot{q}_n(t) + p_n(t) \tag{22}$$

Here we have used the definitions

$$p_n(t) = -\boldsymbol{\phi}_n^{\mathrm{T}}\mathbf{K}_{\mathrm{sb}}\mathbf{u}_{\mathrm{b}}(t), \quad q_n(t) = -\boldsymbol{\phi}_n^{\mathrm{T}}\mathbf{M}_{\mathrm{sb}}\dot{\mathbf{u}}_{\mathrm{b}}(t) \tag{23}$$

We note that $p_n(0) = 0$ and $q_n(0) = 0$ from (4). From (20) and from (4) again we also have

$$Y_n(0) = 0, \quad \dot{Y}_n(0) = 0 \tag{24}$$

To solve (22) and (24) we first find the Green function $g_n(t)$ associated with these equations. This Green function satisfies

$$\ddot{g}_n(t) + \omega_n^2 g_n(t) = \delta(t) \tag{25}$$

$$g_n(0) = 0, \quad \dot{g}_n(0^-) = 0 \tag{26}$$

where $\delta(t)$ is the Dirac delta function. It is easy to verify that the Green function is

$$g_n(t) = \frac{\sin \omega_n t}{\omega_n}, \quad t \geqslant 0 \tag{27}$$

With $g(t)$ known, the solution of (22) and (24) is

$$Y_n(t) = \int_0^t g_n(t-\tau) p_n(\tau)\,\mathrm{d}\tau + \int_0^t g_n(t-\tau)\dot{q}_n(\tau)\,\mathrm{d}\tau \tag{28}$$

We use (27) in (28) and integrate by parts once to obtain

$$Y_n(t) = \frac{p_n(t)}{\omega_n^2} - \int_0^t \frac{\cos \omega_n(t-\tau)}{\omega_n^2}\,\dot{p}_n(\tau)\,\mathrm{d}\tau + \int_0^t \cos \omega_n(t-\tau) q_n(\tau)\,\mathrm{d}\tau \tag{29}$$

Then from (20) and (29) we obtain

$$\mathbf{u}_\mathrm{s}(t) = \sum_{n=1}^{N_\mathrm{s}} \boldsymbol{\phi}_n \left[\frac{p_n(t)}{\omega_n^2} - \int_0^t \cos \omega_n(t-\tau) \left(\frac{\dot{p}_n(\tau)}{\omega_n^2} - q_n(\tau) \right) \mathrm{d}\tau \right] \tag{30}$$

Equation (30) is an expression for $\mathbf{u}_\mathrm{s}$ that we shall use momentarily. We also need an expression for $\ddot{\mathbf{u}}_\mathrm{s}$. From (20) and (22) we find, after some algebra,

$$\ddot{\mathbf{u}}_\mathrm{s} = \sum_{n=1}^{N_\mathrm{s}} \phi_n \left[\int_0^t \cos \omega_n(t-\tau) \left(\dot{p}_n(\tau) - \omega_n^2 q_n(\tau) \right) \mathrm{d}\tau + \dot{q}_n(t) \right] \tag{31}$$

Now the expressions for $p_n(t)$ and $q_n(t)$ given by (23) are used in (30) and (31), and the results are substituted in (10) to evaluate

$$\begin{aligned}
\mathbf{f}_\mathrm{b}(t) = {} & -\mathbf{M}_\mathrm{bb}\ddot{\mathbf{u}}_\mathrm{b}(t) - \mathbf{K}_\mathrm{bb}\mathbf{u}_\mathrm{b}(t) \\
& -\mathbf{M}_\mathrm{bs} \sum_{n=1}^{N_\mathrm{s}} \boldsymbol{\phi}_n \left[\int_0^t \cos \omega_n(t-\tau) \left(-\boldsymbol{\phi}_n^\mathrm{T}\mathbf{K}_\mathrm{sb}\dot{\mathbf{u}}_\mathrm{b} + \omega_n^2 \boldsymbol{\phi}_n^\mathrm{T}\mathbf{M}_\mathrm{sb}\dot{\mathbf{u}}_\mathrm{b} \right) \mathrm{d}\tau - \boldsymbol{\phi}_n^\mathrm{T}\mathbf{M}_\mathrm{sb}\ddot{\mathbf{u}}_\mathrm{b} \right] \\
& -\mathbf{K}_\mathrm{bs} \sum_{n=1}^{N_\mathrm{s}} \boldsymbol{\phi}_n \left[-\frac{\boldsymbol{\phi}_n^\mathrm{T}\mathbf{K}_\mathrm{sb}\mathbf{u}_\mathrm{b}}{\omega_n^2} - \int_0^t \cos \omega_n(t-\tau) \left(-\frac{\boldsymbol{\phi}_n^\mathrm{T}\mathbf{K}_\mathrm{sb}\dot{\mathbf{u}}_\mathrm{b}}{\omega_n^2} + \boldsymbol{\phi}_n^\mathrm{T}\mathbf{M}_\mathrm{sb}\dot{\mathbf{u}}_\mathrm{b} \right) \mathrm{d}\tau \right]
\end{aligned} \tag{32}$$

Finally, we rearrange (32), and recognize that $\sum_{n=1}^{N_s} \boldsymbol{\phi}_n \boldsymbol{\phi}_n^T = \mathbf{M}_{ss}^{-1}$ and $\sum_{n=1}^{N_s} \boldsymbol{\phi}_n \boldsymbol{\phi}_n^T / \omega_n^2 = \mathbf{K}_{ss}^{-1}$, to obtain

$$\mathbf{f}_b(t) = -(\mathbf{M}_{bb} - \mathbf{M}_{bs}\mathbf{M}_{ss}^{-1}\mathbf{M}_{sb})\ddot{\mathbf{u}}_b(t) - (\mathbf{K}_{bb} - \mathbf{K}_{bs}\mathbf{K}_{ss}^{-1}\mathbf{K}_{sb})\mathbf{u}_b(t) - \sum_{n=1}^{N_s} \mathbf{S}_n \int_0^t \cos\omega_n(t-\tau)\dot{\mathbf{u}}_b(\tau)\,\mathrm{d}\tau \tag{33}$$

Here $\mathbf{S}_n$ is the $N_b \times N_b$ matrix which we call *the coupling matrix* for the nth mode and which is defined by

$$\mathbf{S}_n = \omega_n^2 \mathbf{M}_{bs}\boldsymbol{\phi}_n\boldsymbol{\phi}_n^T\mathbf{M}_{sb} - \mathbf{M}_{bs}\boldsymbol{\phi}_n\boldsymbol{\phi}_n^T\mathbf{K}_{sb} - \mathbf{K}_{bs}\boldsymbol{\phi}_n\boldsymbol{\phi}_n^T\mathbf{M}_{sb} + \frac{1}{\omega_n^2}\mathbf{K}_{bs}\boldsymbol{\phi}_n\boldsymbol{\phi}_n^T\mathbf{K}_{sb} \tag{34}$$

By looking at its form it is obvious that the matrix $\mathbf{S}_n$ is related to the coupling between the interface 'b' and the subsystem 's' for the nth mode, hence its name. It is easy to see that this is a symmetric rank-1 matrix, as follows. We let

$$\mathbf{s}_n = \omega_n \mathbf{M}_{bs}\boldsymbol{\phi}_n - \frac{1}{\omega_n}\mathbf{K}_{bs}\boldsymbol{\phi}_n \tag{35}$$

Then

$$\mathbf{S}_n = \mathbf{s}_n\mathbf{s}_n^T \tag{36}$$

In writing (33), we have assumed that the matrices $\mathbf{M}_{ss}$ and $\mathbf{K}_{ss}$ are non-singular. This indeed follows from our assumption that they are symmetric and positive definite.

An exactly analogous calculation can be performed for the reduced subsystem. The end result can easily be deduced from (33) by simply replacing each matrix with its counterpart in the reduced subsystem:

$$\tilde{\mathbf{f}}_b(t) = -(\mathbf{m}_{bb} - \mathbf{m}_{br}\mathbf{m}_{ss}^{-1}\mathbf{m}_{rb})\ddot{\mathbf{u}}_b(t) - (\mathbf{k}_{bb} - \mathbf{k}_{br}\mathbf{k}_{ss}^{-1}\mathbf{k}_{rb})\mathbf{u}_b(t) - \sum_{n=1}^{N_r} \tilde{\mathbf{S}}_n \int_0^t \cos\tilde{\omega}_n(t-\tau)\dot{\mathbf{u}}_b(\tau)\,\mathrm{d}\tau \tag{37}$$

Here $\tilde{\mathbf{S}}_n$ is the $N_b \times N_b$ coupling matrix for the reduced subsystem whose definition is analogous to (34), i.e.

$$\tilde{\mathbf{S}}_n = \tilde{\omega}_n^2 \mathbf{m}_{br}\tilde{\boldsymbol{\phi}}_n\tilde{\boldsymbol{\phi}}_n^T\mathbf{m}_{rb} - \mathbf{m}_{br}\tilde{\boldsymbol{\phi}}_n\tilde{\boldsymbol{\phi}}_n^T\mathbf{k}_{rb} - \mathbf{k}_{br}\tilde{\boldsymbol{\phi}}_n\tilde{\boldsymbol{\phi}}_n^T\mathbf{m}_{rb} + \frac{1}{\tilde{\omega}_n^2}\mathbf{k}_{br}\tilde{\boldsymbol{\phi}}_n\tilde{\boldsymbol{\phi}}_n^T\mathbf{k}_{rb} \tag{38}$$

The $\tilde{\omega}_n$ and $\tilde{\boldsymbol{\phi}}_n$ are, respectively, the eigenfrequencies and eigenvectors of the generalized eigenvalue problem associated with the reduced subsystem, i.e.

$$\mathbf{k}_{rr}\tilde{\boldsymbol{\phi}} = \tilde{\omega}^2\mathbf{m}_{rr}\tilde{\boldsymbol{\phi}} \tag{39}$$

In writing (37), we have assumed that $\mathbf{m}_{rr}^{-1}$ and $\mathbf{k}_{rr}^{-1}$ exist. Indeed this is the case, as will become clear in the next section.

4. THE OPTIMAL MODAL REDUCTION ALGORITHM

We now concentrate on *modal reduction*. To this end, we truncate expansion (20) of $\mathbf{u}_s$ after N_r terms. Namely, we replace (20) by the approximation

$$\mathbf{u}_s(t) \simeq \sum_{n=1}^{N_r} \tilde{\boldsymbol{\phi}}_n y_n(t) \equiv \boldsymbol{\Phi}_r \mathbf{y}(t) \tag{40}$$

Here $\boldsymbol{\Phi}_r = [\tilde{\boldsymbol{\phi}}_n]$ is the $N_s \times N_r$ matrix whose columns are the N_r 'most important' eigenvectors chosen out of the N_s eigenvectors ϕ_n of the original subsystem. We shall soon see how those N_r modes are chosen.

Now, we consider Equation (19) again, describing the original subsystem:

$$\mathbf{M}_{ss}\ddot{\mathbf{u}}_s + \mathbf{K}_{ss}\mathbf{u}_s = -\mathbf{M}_{sb}\ddot{\mathbf{u}}_b - \mathbf{K}_{sb}\mathbf{u}_b \tag{41}$$

To reduce this set of N_s equations into a set of N_r equations, we multiply both sides of (41) on the left by $\boldsymbol{\Phi}_r^T$. Then we substitute (40) in the resulting equation, which yields

$$(\boldsymbol{\Phi}_r^T\mathbf{M}_{ss}\boldsymbol{\Phi}_r)\ddot{\mathbf{y}} + (\boldsymbol{\Phi}_r^T\mathbf{K}_{ss}\boldsymbol{\Phi}_r)\mathbf{y} = -\boldsymbol{\Phi}_r^T\mathbf{M}_{sb}\ddot{\mathbf{u}}_b - \boldsymbol{\Phi}_r^T\mathbf{K}_{sb}\mathbf{u}_b \tag{42}$$

Using the orthogonality properties of the eigenvectors (cf. (17) and (18)) we obtain

$$\ddot{\mathbf{y}} + \boldsymbol{\Omega}_r^2\mathbf{y} = -\boldsymbol{\Phi}_r^T\mathbf{M}_{sb}\ddot{\mathbf{u}}_b - \boldsymbol{\Phi}_r^T\mathbf{K}_{sb}\mathbf{u}_b \tag{43}$$

Here $\boldsymbol{\Omega}_r^2$ is the $N_r \times N_r$ diagonal matrix whose diagonal entries are the squared frequencies of the N_r chosen modes.

On the other hand, the third set of equations in (5) describes the reduced subsystem 'r', i.e.

$$\mathbf{m}_{rr}\ddot{\mathbf{u}}_r + \mathbf{k}_{rr}\mathbf{u}_r = -\mathbf{m}_{rb}\ddot{\mathbf{u}}_b - \mathbf{k}_{rb}\mathbf{u}_b \tag{44}$$

Comparing (44) with (43), we identify $\mathbf{y}(t)$ with $\mathbf{u}_r(t)$ and deduce

$$\mathbf{m}_{rr} = \mathbf{I}_r \tag{45}$$

$$\mathbf{k}_{rr} = \boldsymbol{\Omega}_r^2 \tag{46}$$

$$\mathbf{m}_{rb} = \mathbf{m}_{br}^T = \boldsymbol{\Phi}_r^T\mathbf{M}_{sb} \tag{47}$$

$$\mathbf{k}_{rb} = \mathbf{k}_{br}^T = \boldsymbol{\Phi}_r^T\mathbf{K}_{sb} \tag{48}$$

Here $\mathbf{I}_r$ is the $N_r \times N_r$ identity. It is easy to show that the matrices $\mathbf{m}_{rr}$ and $\mathbf{k}_{rr}$ obtained by (45) and (46) are symmetric and positive definite. In other words, the reduced matrices $\mathbf{m}_{rr}$ and $\mathbf{k}_{rr}$ inherit the properties of the original matrices $\mathbf{M}_{ss}$ and $\mathbf{K}_{ss}$.

Having determined the matrices $\mathbf{m}_{rr}$, $\mathbf{k}_{rr}$, $\mathbf{m}_{rb}$ and $\mathbf{k}_{rb}$, it remains to determine the matrices $\mathbf{m}_{bb}$ and $\mathbf{k}_{bb}$ and to decide which of the original N_s modes is to be included in the reduced list of N_r modes. To address both these issues, we recall that the goal is to minimize $\Pi \equiv \|\mathbf{f}_b - \tilde{\mathbf{f}}_b\|_T$

as defined by (12). We take the difference between (33) and (37) to obtain

$$\mathbf{f}(t) - \tilde{\mathbf{f}}(t) = \mathbf{M}_0\ddot{\mathbf{u}}_\mathrm{b} + \mathbf{K}_0\mathbf{u}_\mathrm{b} - \sum_{n=1}^{N_\mathrm{s}} \mathbf{S}_n \int_0^t \cos\omega_n(t-\tau)\dot{\mathbf{u}}_\mathrm{b}(\tau)\,\mathrm{d}\tau$$
$$+ \sum_{n=1}^{N_\mathrm{r}} \tilde{\mathbf{S}}_n \int_0^t \cos\tilde{\omega}_n(t-\tau)\dot{\mathbf{u}}_\mathrm{b}(\tau)\,\mathrm{d}\tau \tag{49}$$

Here

$$\mathbf{M}_0 = -(\mathbf{M}_\mathrm{bb} - \mathbf{M}_\mathrm{bs}\mathbf{M}_\mathrm{ss}^{-1}\mathbf{M}_\mathrm{sb}) + (\mathbf{m}_\mathrm{bb} - \mathbf{m}_\mathrm{br}\mathbf{m}_\mathrm{rr}^{-1}\mathbf{m}_\mathrm{rb}) \tag{50}$$

$$\mathbf{K}_0 = -(\mathbf{K}_\mathrm{bb} - \mathbf{K}_\mathrm{bs}\mathbf{K}_\mathrm{ss}^{-1}\mathbf{K}_\mathrm{sb}) + (\mathbf{k}_\mathrm{bb} - \mathbf{k}_\mathrm{br}\mathbf{k}_\mathrm{rr}^{-1}\mathbf{k}_\mathrm{rb}) \tag{51}$$

Since we achieve the reduction via modal truncation, then by construction $\tilde{\omega}_n = \omega_n$ for $n = 1, \ldots, N_\mathrm{r}$. From this we can also deduce that $\tilde{\mathbf{S}}_n = \mathbf{S}_n$ for $n = 1, \ldots, N_\mathrm{r}$ (see Appendix A). Thus, (49) reduces to

$$\mathbf{f}(t) - \tilde{\mathbf{f}}(t) = \mathbf{M}_0\ddot{\mathbf{u}}_\mathrm{b} + \mathbf{K}_0\mathbf{u}_\mathrm{b} - \sum_{n=N_\mathrm{r}+1}^{N_\mathrm{s}} \mathbf{S}_n \int_0^t \cos\omega_n(t-\tau)\dot{\mathbf{u}}_\mathrm{b}(\tau)\,\mathrm{d}\tau \tag{52}$$

Now we can estimate

$$\Pi \equiv \|\mathbf{f}_\mathrm{b} - \tilde{\mathbf{f}}_\mathrm{b}\|_T \leqslant \|\mathbf{M}_0\ddot{\mathbf{u}}_\mathrm{b} + \mathbf{K}_0\mathbf{u}_\mathrm{b}\|_T + \sum_{n=N_\mathrm{r}+1}^{N_\mathrm{s}} \|\mathbf{S}_n\| \left\| \int_0^t \cos\omega_n(t-\tau)\dot{\mathbf{u}}_\mathrm{b}(\tau)\,\mathrm{d}\tau \right\|_T \tag{53}$$

Here $\|\mathbf{S}_n\|$ is the norm of the coupling matrix $\mathbf{S}_n$; this can be either the Frobenius norm defined by

$$\|\mathbf{S}\| = \left(\sum_{i=1}^{N_\mathrm{b}} \sum_{j=1}^{N_\mathrm{b}} S_{ij}^2 \right)^{1/2} \tag{54}$$

or the 2-norm $\|\cdot\|_2$ induced by the Euclidian vector norm; see, e.g. Reference [22]. In fact, since $\mathbf{S}_n$ is a symmetric rank-one matrix (cf. (36)), it can be shown that the two norms are identical in this case.

The first norm on the right-hand side of (53) can be minimized by simply taking $\mathbf{M}_0 = \mathbf{0}$ and $\mathbf{K}_0 = \mathbf{0}$. From (50) and (51), this choice yields expressions for $\mathbf{m}_\mathrm{bb}$ and $\mathbf{k}_\mathrm{bb}$, i.e.

$$\mathbf{m}_\mathrm{bb} = \mathbf{M}_\mathrm{bb} - \mathbf{M}_\mathrm{bs}\mathbf{M}_\mathrm{ss}^{-1}\mathbf{M}_\mathrm{sb} + \mathbf{m}_\mathrm{br}\mathbf{m}_\mathrm{rr}^{-1}\mathbf{m}_\mathrm{rb} \tag{55}$$

$$\mathbf{k}_\mathrm{bb} = \mathbf{K}_\mathrm{bb} - \mathbf{K}_\mathrm{bs}\mathbf{K}_\mathrm{ss}^{-1}\mathbf{K}_\mathrm{sb} + \mathbf{k}_\mathrm{br}\mathbf{k}_\mathrm{rr}^{-1}\mathbf{k}_\mathrm{rb} \tag{56}$$

Note that all the matrices on the right-hand sides of (55) and (56) are known, being either the submatrices comprising the original subsystem, or the submatrices of the reduced subsystem that have already been found (see (45)–(48)).

Having chosen $\mathbf{M}_0 = \mathbf{0}$ and $\mathbf{K}_0 = \mathbf{0}$, it now remains to minimize the sum on the right-hand side of (53). This term depends on the function $\dot{\mathbf{u}}_\mathrm{b}$ which is, of course, unknown. For an arbitrary $\dot{\mathbf{u}}_\mathrm{b}$, the best that we can do is to minimize the coefficients $\|\mathbf{S}_n\|$ for $n = N_\mathrm{r}+1, \ldots, N_\mathrm{s}$. Thus, among the N_s modes of the original subsystem, the modes $n = N_\mathrm{r} + 1, \ldots, N_\mathrm{s}$ should be those for which the corresponding matrices $\mathbf{S}_n$ have the smallest norms. This yields the rule for choosing the first N_r '*important*' *modes*: *these are the modes for which the corresponding coupling matrices* $\mathbf{S}_n$ *have the largest norms*.

The estimate in (53) which leads to the $\|\mathbf{S}_n\|$-based criterion is taken in order that the reduction be accurate for a wide variety of responses. The resulting reduction is optimal in the sense that no better reduction may be found for arbitrary loads and initial conditions.

We can now assemble all the pieces derived above into a single algorithm which we call *optimal modal reduction* (*OMR*). The OMR algorithm is summarized in Box 1.

Box 1. The OMR algorithm.

- Given: the matrices $\mathbf{M}_\mathrm{bb}$, $\mathbf{M}_\mathrm{ss}$, $\mathbf{M}_\mathrm{bs} = \mathbf{M}_\mathrm{sb}^\mathrm{T}$, $\mathbf{K}_\mathrm{bb}$, $\mathbf{K}_\mathrm{ss}$ and $\mathbf{K}_\mathrm{bs} = \mathbf{K}_\mathrm{sb}^\mathrm{T}$ in (3).
- Solve the generalized eigenvalue problem

$$\mathbf{K}_\mathrm{ss}\boldsymbol{\phi} = \omega^2\mathbf{M}_\mathrm{ss}\boldsymbol{\phi}$$

  and find the N_s eigenfrequencies ω_n and corresponding eigenvectors $\boldsymbol{\phi}_n$. Normalize the eigenvectors such that $\boldsymbol{\phi}_n^\mathrm{T}\mathbf{M}_\mathrm{ss}\boldsymbol{\phi}_n = 1$.
- For each mode $n = 1, \ldots, N_\mathrm{s}$, calculate $\|\mathbf{S}_n\|$ by using (34) and (54).
- Sort the modes according to the value of $\|\mathbf{S}_n\|$ in descending order. Thus,

$$\|\mathbf{S}_1\| \geqslant \|\mathbf{S}_2\| \geqslant \cdots \geqslant \|\mathbf{S}_{N_\mathrm{s}}\|$$

- If the dimension of the reduced subsystem, N_r, is not given *a priori*, Choose N_r. A reasonable way to do this is to take N_r such that $\|\mathbf{S}_{N_\mathrm{r}}\| \simeq \alpha\|\mathbf{S}_1\|$, where $0 < \alpha < 1$ is a given parameter. In other words, choose N_r so that the minimum $\|\mathbf{S}_n\|$ value of the retained modes is a given fraction (say $\alpha = 30\%$) of the maximum $\|\mathbf{S}_n\|$ value.
- Let $\mathbf{I}_\mathrm{r}$ be the $N_\mathrm{r} \times N_\mathrm{r}$ identity, $\boldsymbol{\Omega}_\mathrm{r}^2$ be the $N_\mathrm{r} \times N_\mathrm{r}$ diagonal matrix whose diagonal entries are the squared frequencies ω_n^2 of the first N_r modes, and $\boldsymbol{\Phi}_\mathrm{r}$ be the $N_\mathrm{s} \times N_\mathrm{r}$ matrix whose columns are the first N_r eigenvectors $\boldsymbol{\phi}_n$. Then

$$\mathbf{m}_\mathrm{rr} = \mathbf{I}_\mathrm{r}, \quad \mathbf{m}_\mathrm{rb} = \mathbf{m}_\mathrm{br}^\mathrm{T} = \boldsymbol{\Phi}_\mathrm{r}^\mathrm{T}\mathbf{M}_\mathrm{sb}$$

$$\mathbf{k}_\mathrm{rr} = \boldsymbol{\Omega}_\mathrm{r}^2, \quad \mathbf{k}_\mathrm{rb} = \mathbf{k}_\mathrm{br}^\mathrm{T} = \boldsymbol{\Phi}_\mathrm{r}^\mathrm{T}\mathbf{K}_\mathrm{sb}$$

- Calculate:

$$\mathbf{m}_\mathrm{bb} = \mathbf{M}_\mathrm{bb} - \mathbf{M}_\mathrm{bs}\mathbf{M}_\mathrm{ss}^{-1}\mathbf{M}_\mathrm{sb} + \mathbf{m}_\mathrm{br}\mathbf{m}_\mathrm{rr}^{-1}\mathbf{m}_\mathrm{rb}$$

$$\mathbf{k}_\mathrm{bb} = \mathbf{K}_\mathrm{bb} - \mathbf{K}_\mathrm{bs}\mathbf{K}_\mathrm{ss}^{-1}\mathbf{K}_\mathrm{sb} + \mathbf{k}_\mathrm{br}\mathbf{k}_\mathrm{rr}^{-1}\mathbf{k}_\mathrm{rb}$$

- The reduced system is (5), with the matrices $\mathbf{m}_\mathrm{bb}$, $\mathbf{m}_\mathrm{br} = \mathbf{m}_\mathrm{rb}^\mathrm{T}$, $\mathbf{m}_\mathrm{rr}$, $\mathbf{k}_\mathrm{bb}$, $\mathbf{k}_\mathrm{br} = \mathbf{k}_\mathrm{rb}^\mathrm{T}$ and $\mathbf{k}_\mathrm{rr}$ obtained above.

We note that OMR differs from standard modal reduction (SMR) in two ways:

1. The rule of 'modal importance' obtained here is different than that used in SMR.
2. The OMR algorithm involves a special construction of the matrices $\mathbf{m}_{\mathrm{bb}}$ and $\mathbf{k}_{\mathrm{bb}}$ as in (55) and (56). In SMR, one usually takes $\mathbf{m}_{\mathrm{bb}} = \mathbf{M}_{\mathrm{bb}}$ and $\mathbf{k}_{\mathrm{bb}} = \mathbf{K}_{\mathrm{bb}}$.

5. PHYSICAL INTERPRETATION

As observed above, the rule of 'modal importance' obtained in OMR is different than that used in SMR, say in structural dynamics. In the latter, the important modes, which are retained in the reduction, are defined to be those with the smallest frequencies. Indeed, various arguments can be given to support the sensibility of the low-frequency rule in the case where the reduction of a complete independent dynamical system is sought. However, when we focus our attention on the reduction of a *subsystem*, it turns out that this rule is not optimal.

The new optimal rule is not based directly on the spectrum of the subsystem as in SMR. Instead, it is based on the *strength of interaction between the subsystem* 's' *and the interface* 'b'. This is manifested mathematically by the way in which the matrices $\mathbf{M}_{\mathrm{bs}}$, $\mathbf{M}_{\mathrm{sb}}$, $\mathbf{K}_{\mathrm{bs}}$ and $\mathbf{K}_{\mathrm{sb}}$ appear in expression (34) for the coupling matrix $\mathbf{S}_n$. According to this new criterion, the important subsystem modes are those that interact strongly with the interface, and thus will potentially affect the main system the most.

To demonstrate this criterion, we consider the set-up illustrated in Figure 2. This example was also examined in Reference [13], in a simplified setting using partial mass lumping. We consider the lateral motion of a linear flat membrane, governed by the scalar wave equation

$$c^2\nabla^2 u = \ddot{u} \tag{57}$$

where u is the lateral displacement and c is the given wave speed. We take $c = 1$. As Figure 2 shows, the main structure is the 3×3 square ACDK, and the attached substructure is the hexagon EFGHIJ. The interface between them is the segment EJ. The sides AC, DE, EF, HI, IJ and JK are fixed (they are represented by thick lines in Figure 2), whereas all the other sides are free. The shaded strip shown in Figure 2 has to do with the initial conditions which will be described later.

We discretize the entire membrane by square bilinear finite elements of size 0.1×0.1. Altogether there are $N = 1988$ degrees of freedom in the discrete membrane (which is the number of nodes excluding the fixed nodes). Of these, there are $N_{\mathrm{b}} = 9$ degrees of freedom on the interface 'b' and $N_{\mathrm{s}} = 1080$ degrees of freedom inside the substructure 's'.

We solve the generalized eigenvalue problem (14) associated with the subsystem 's'. Then we sort all the eigenmodes in two different ways: by ascending frequencies (SMR) and by descending $\|\mathbf{S}_n\|$ norm values (OMR). Table I shows the characteristics of the first 10 modes according to the SMR sorting. For each mode number n the values of $\|\mathbf{S}_n\|$ and the frequency ω_n are given in the table. In addition, the last column indicates the position of this mode in the list generated by using OMR sorting. Table II describes the first 10 modes according to the OMR sorting. Its last column indicates the position of each mode in the list generated by using SMR sorting.

By inspecting Tables I and II we observe that the two top-ten sets of modes obtained in SMR and OMR are completely disjoint. Moreover, some of the modes that appear in one of

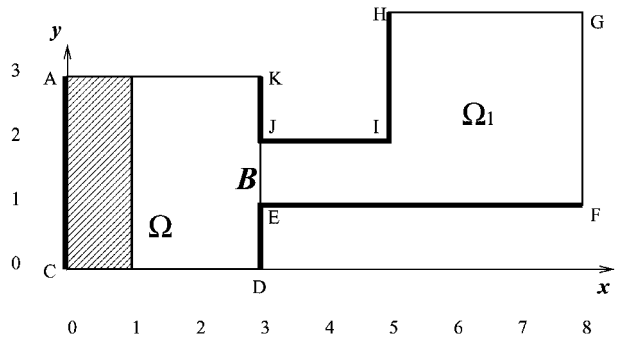

Figure 2. The vibrating membrane problem.

Table I. Top-ten modes according to SMR (i.e. modes are sorted by ascending frequencies). The last column shows for each mode its position in the OMR list.

SMR-mode number n	$\|\mathbf{S}_n\|$	Frequency	Mode number in OMR-mode list
1	3.73×10^{-17}	0.74	1071
2	8.95×10^{-15}	1.65	1062
3	2.09×10^{-24}	1.66	1078
4	1.26×10^{-12}	2.20	1027
5	2.36×10^{-11}	2.66	942
6	1.17×10^{-19}	2.68	1073
7	1.59×10^{-8}	2.95	527
8	9.50×10^{-16}	3.06	1068
9	4.30×10^{-5}	3.36	89
10	7.84×10^{-5}	3.64	54

the top-ten list are found in the middle or even at the end of the other full list. For example, the single most important mode according to SMR is number 1071 (out of 1080 total) in the OMR list. Thus, the two criteria for 'modal importance' lead to completely different results. This is also seen in Figure 3, which shows the frequencies of the OMR-sorted modes (joined by straight lines) as a function of the mode number. Although there is a general correlation between the OMR-mode number and the frequency, there are many exceptions which make the dependence between the two highly non-monotone. Note in particular the long 'spikes' seen in Figure 3 for large n; these correspond to modes which are regarded as unimportant in OMR, but whose frequencies are low and are thus considered very important in SMR. A concern with OMR is that it may include 'high frequency' modes which are not accurately discretized. If so, this can be an indication that the original FEM discretization is not accurately capturing all the important physical phenomena in a given problem.

To better understand the difference between the two 'modal importance' criteria, we visualize the first eigenfunction obtained in SMR and in OMR in Figures 4 and 5, respectively. This

Table II. Top-ten modes according to OMR (i.e. modes are sorted by descending $\|\mathbf{S}_n\|$ values). The last column shows for each mode its position in the SMR list.

OMR-mode number n	$\|\mathbf{S}_n\|$	Frequency	Mode number in SMR-mode list
1	37.79×10^5	9.13	66
2	35.96×10^5	8.50	60
3	35.19×10^5	28.67	528
4	34.15×10^5	11.18	99
5	32.64×10^5	5.50	25
6	30.05×10^5	7.72	49
7	28.19×10^5	11.07	98
8	26.83×10^5	5.93	28
9	26.25×10^5	6.58	35
10	25.95×10^5	8.62	61

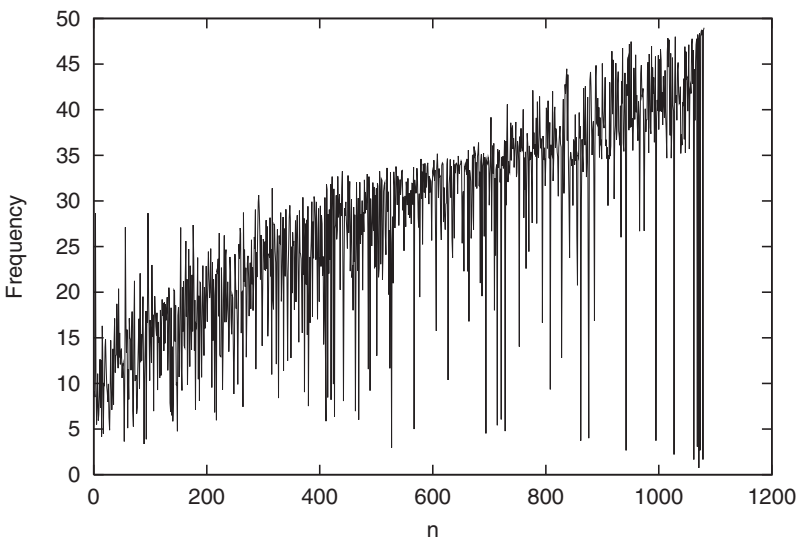

Figure 3. Frequencies of the OMR-sorted modes (joined by straight lines) as a function of the mode number.

eigenfunction is obtained, via finite element interpolation, from the corresponding eigenvector $\boldsymbol{\phi}_1$, whose entries are the nodal values of the first mode. Both the colours and the contour lines in Figures 4 and 5 represent values of u. The first SMR mode, shown in Figure 4, has by construction the lowest frequency among all the modes of the subsystem ($\omega_1 = 0.74$; see Table I). The first OMR mode, shown in Figure 5, has a much higher frequency ($\omega_1 = 9.13$; see Table II), but, by definition, its coupling matrix has the largest norm. The difference

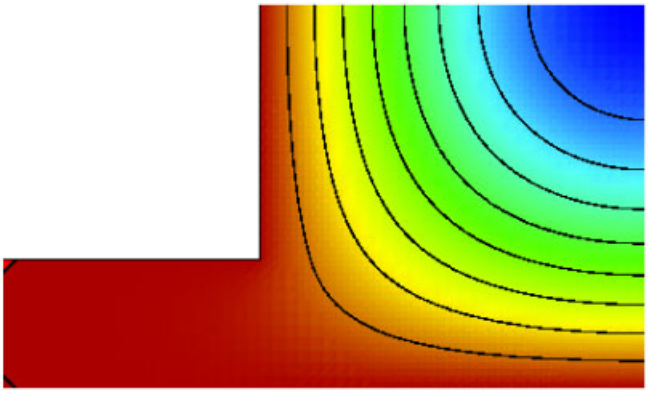

Figure 4. The first subsystem eigenfunction, ϕ_1, obtained by SMR. The eigenfunction is plotted over the domain of the substructure 's'. The left side of this domain is the interface 'b' connecting 's' to the main structure 'm' which is not shown. Both the colours and the contour lines represent values of u.

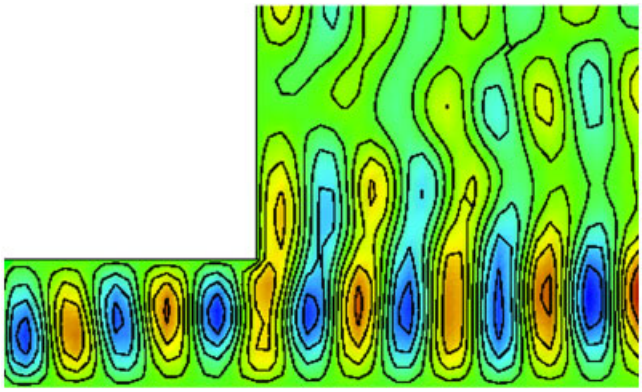

Figure 5. The first subsystem eigenfunction, ϕ_1, obtained by OMR. The eigenfunction is plotted over the domain of the substructure 's'. The left side of this domain is the interface 'b' connecting 's' to the main structure 'm' which is not shown. Both the colours and the contour lines represent values of u.

between the two modes is seen very clearly by comparing the two figures; while the SMR mode illustrated in Figure 4 is 'global' and smooth, the OMR mode in Figure 5 is rapidly oscillating.

We have already argued that the strength of the coupling between the subsystem and the main system, which is the measure used by the OMR criterion, manifests itself in the forces that the subsystem 's' applies on the interface 'b'. For finite elements with uniform stiffness (i.e. elements with the same size and material properties, as in the present case), these forces are proportional to the *gradients* of u along the interface. Thus, we can visualize the strength of system–subsystem coupling of the two modes shown in Figures 4 and 5 by looking at the

changes of colour or at the density of contours near the interface in these two figures. It is clear that the SMR mode (Figure 4) is associated with very weak coupling, whereas the OMR mode (Figure 5) exhibits strong coupling. There is no point in retaining the first SMR mode in the reduced subsystem, since it has hardly any effect on the main system whose dynamical behaviour is of interest to us. On the other hand, the first OMR mode plays an important role in this dynamical behaviour and therefore must not be omitted, despite the fact that its frequency is rather high.

6. NUMERICAL RESULTS

We now solve the vibrating membrane problem introduced above as a time-dependent problem. To this end we need to specify initial conditions. The initial velocity is zero everywhere. The initial displacement is also zero everywhere except in the left shaded 3×1 strip shown in Figure 2. In this strip the initial displacement is a 'hat' function, changing linearly from $u = 0$ along the line $x = 0$ to $u = 1$ along the lines $x = 0.5$ to $u = 0$ again along the line $x = 1$. We use the Newmark trapezoidal time-integration scheme [23] with time-step increment $\Delta t = 0.01$ to solve both the original problem (3) and the reduced problem (5) with the given initial conditions.

The geometry, boundary conditions and initial conditions of this problem guarantee a complicated solution. The initial pulse propagates to the right with speed $c = 1$, penetrates the substructure and is reflected back to the main structure from the substructure walls as well as the from the boundaries DE and JK. There are many reflections, including internal reflections among the walls of the substructure. Moreover, there is a geometrical wave dispersion effect due to fact that the domain has the shape of a wave guide. Thus, the solution consists of complex wave patterns that involve significant modes with both low and high frequencies. During the simulation time the wave travels a number of times the entire length of the membrane.

How many modes (or degrees of freedom) should we include in the reduced substructure, namely what is a good choice for N_r? In Box 1, we have proposed a simple procedure for determining N_r. To see how this procedure should be applied in the present example, we plot in Figure 6 the graph of $\|\mathbf{S}_n\|$ as a function of n ($1 \leqslant n \leqslant N_s = 1080$), after OMR mode sorting. We see that at about $n = 200$ the graph starts to level off. Thus, a reduced model with $N_r = 200$ is a very reasonable choice in this case. This amounts to a great reduction in the number of degrees of freedom, namely a reduction of $(N_s - N_r)/N_s = 81.5\%$. We have tried a number of reduced models, with N_r varying between 1 and 200.

First, the dimension of the reduced subsystem is chosen to be $N_r = 50$. Since the dimension of the original subsystem is $N_s = 1080$, this yields a reduction of $N_r/N_s = 95.4\%$. Figures 7(a) and (b) show the solution u as a function of x for $y = 1.5$ at two times: $t = 4$ and 25. Note that the x range shown is that which is in the main system 's', since there is no interest in the accuracy of the solution inside the subsystem. We compare three solutions in each figure: the solution for the original substructure ($N_r = N_s = 1080$), the solution for the reduced substructure with $N_r = 50$ obtained by OMR, and the solution with $N_r = 50$ obtained by SMR. The deviations of both the SMR and OMR solutions from the full-model solution grow in time, but the deviation of the SMR solution is much larger. In general the OMR solution remains close to the full solution, whereas the SMR solution is far off.

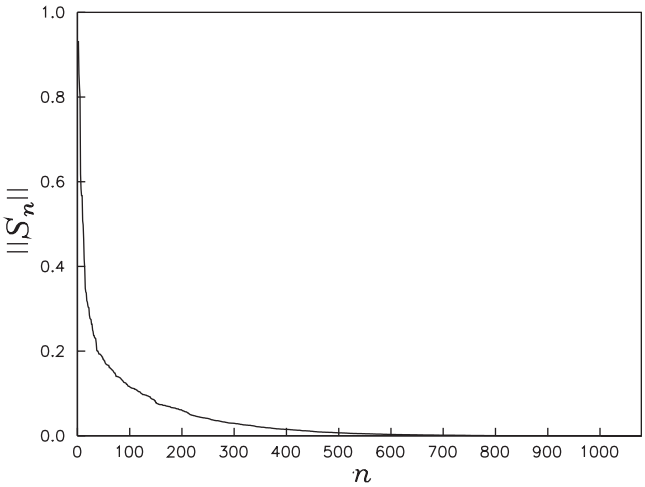

Figure 6. The norm of the coupling matrix, $\|\mathbf{S}_n\|$, as a function of the mode number n, after OMR mode sorting.

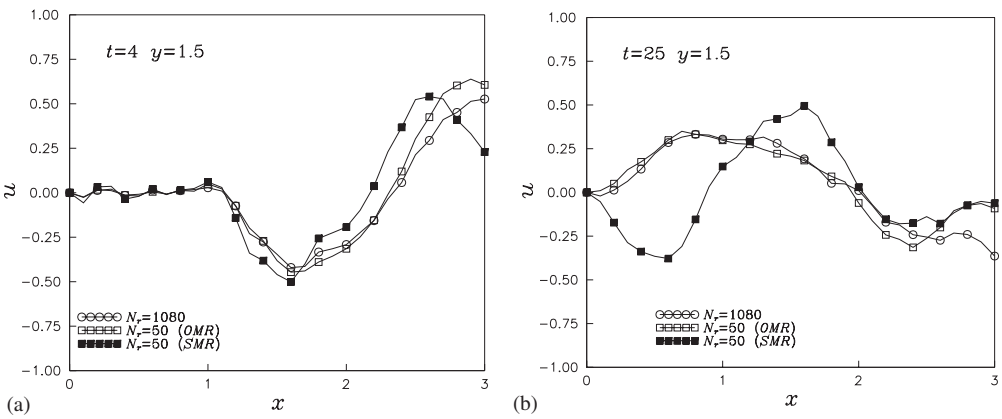

Figure 7. Solution u as a function of x for $y = 1.5$ for the full model ($N_\mathrm{r} = N_\mathrm{s} = 1080$), the reduced model with $N_\mathrm{r} = 50$ using OMR, and the reduced model with $N_\mathrm{r} = 50$ using SMR, at times: (a) $t = 4$; and (b) $t = 25$.

To examine the local accuracy more closely, we define the relative pointwise error

$$e(t) = \|u(x, y, t) - \tilde{u}(x, y, t)\|_0 / \|u(x, y, t)\|_0 \tag{58}$$

where u is the full solution ($N_\mathrm{r} = 1080$), $\tilde{u}$ is the reduced solution, and $\|\cdot\|_0$ is the one-dimensional L_2 norm along the middle horizontal 'fibre' in the main structure, i.e. along the segment $y = 1.5$, $0 \leqslant x \leqslant 3$. Figure 8(a) shows the error $e(t)$ generated by the OMR scheme with different numbers of degrees of freedom N_r, on a logarithmic scale. The critical deterioration between $N_\mathrm{r} = 30$ and 10 is evident. We also see that although the error has an

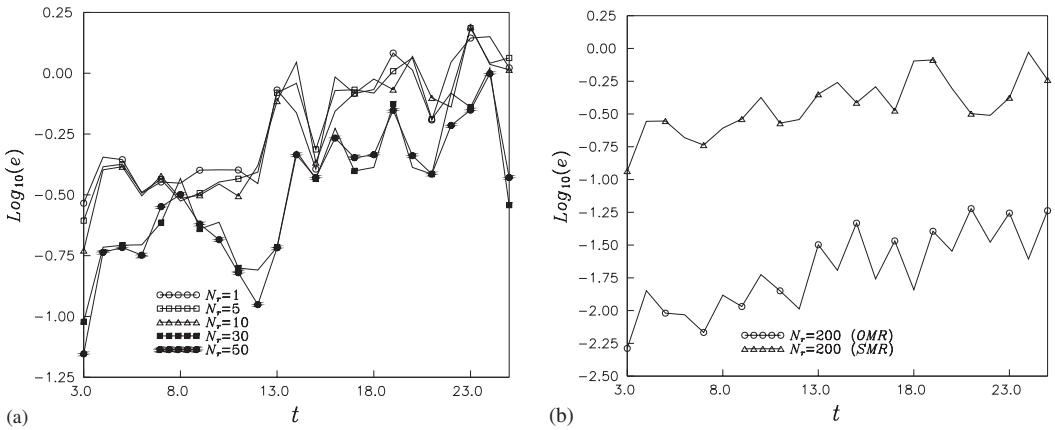

Figure 8. The relative error $e(t)$: (a) comparison of the errors generated by OMR with reduced models having $N_r = 1$, 5, 10, 30 and 50 degrees of freedom; and (b) comparison between the errors generated OMR and by SMR with $N_r = 200$ degrees of freedom.

oscillatory behaviour it generally increases in time. Figure 8(b) compares the OMR error to the SMR error, for $N_r = 200$. The general superiority of OMR is clear. In fact, the OMR error is more than an order of magnitude smaller than the SMR error.

The example shown was chosen to demonstrate clearly the potential advantage of OMR to SMR when one is interested in the effect one part of a system has on another. It is expected that such clear superiority will not be evidenced in every possible example. In fact, in an experiment done with a simple rectangular domain (with a Dirichlet condition along its entire boundary) which was subdivided into two rectangular domains (the main system and the subsystem), OMR and SMR yielded very similar results.

Figure 3 provides evidence supporting the rule of thumb that lower-frequency modes tend to be more important than higher-frequency modes. This may explain why SMR tends to give satisfactory, if *suboptimal*, results. Figure 3 shows also that this rule of thumb is not generally true. The OMR criterion, on the other hand, generally provides an *optimal* reduction, and thus should be viewed as an important tool in the armory of the analyser.

7. CONCLUDING REMARKS

We have proposed a new criterion for choosing the modes to be retained in the reduction of a linear dynamical subsystem. We have shown how this criterion can be incorporated in an effective algorithm of optimal modal reduction (OMR). The important modes of the subsystem turned out to be those whose coupling matrices have the highest norm. The new formulation is an extension of the partially lumped scheme presented in Reference [13].

We intend to combine the new OMR scheme with the 'high modal density' approximation devised in Reference [19]. The latter is a very effective way to represent subsystems in problems where the modes are dense, namely packed in near each other, a situation which arises in a number of important applications.

As we have remarked in the end of Section 4, the OMR scheme is different than standard modal reduction (SMR) in more than just the rule of 'modal importance'. A second difference is related to the special construction of the matrices $\mathbf{m}_{\mathrm{bb}}$ and $\mathbf{k}_{\mathrm{bb}}$ (see Box 1, or (55) and (56)). We have not discussed this aspect of the OMR scheme in detail in this paper; this has been done in Reference [13] in the context of the partially-lumped formulation. This special construction of the interface matrices turns out to be about as important as implementing the 'modal importance' rule.

APPENDIX A. PROOF THAT $\tilde{\mathbf{S}}_n = \mathbf{S}_n$ FOR $n = 1, \ldots, N_{\mathrm{r}}$

By construction,

$$\tilde{\omega}_n = \omega_n \quad \text{for } n = 1, \ldots, N_r \tag{A1}$$

From this fact and from (45), (46) and (39), we deduce that the eigenvectors $\tilde{\boldsymbol{\phi}}_n$ are just the Cartesian unit vectors. Therefore,

$$\boldsymbol{\Phi}_{\mathrm{r}}\tilde{\boldsymbol{\phi}}_n = \boldsymbol{\phi}_n \tag{A2}$$

Now, we substitute expressions (47) and (48) for $\mathbf{m}_{\mathrm{br}}$ and $\mathbf{k}_{\mathrm{br}}$ in (38) to obtain

$$\begin{aligned}\tilde{\mathbf{S}}_n = {} & \tilde{\omega}_n^2\mathbf{M}_{\mathrm{bs}}\boldsymbol{\Phi}_{\mathrm{r}}\tilde{\boldsymbol{\phi}}_n\tilde{\boldsymbol{\phi}}_n^{\mathrm{T}}\boldsymbol{\Phi}_{\mathrm{r}}^{\mathrm{T}}\mathbf{M}_{\mathrm{sb}} - \mathbf{M}_{\mathrm{bs}}\boldsymbol{\Phi}_{\mathrm{r}}\tilde{\boldsymbol{\phi}}_n\tilde{\boldsymbol{\phi}}_n^{\mathrm{T}}\boldsymbol{\Phi}_{\mathrm{r}}^{\mathrm{T}}\mathbf{K}_{\mathrm{sb}} \\ & -\mathbf{K}_{\mathrm{bs}}\boldsymbol{\Phi}_{\mathrm{r}}\tilde{\boldsymbol{\phi}}_n\tilde{\boldsymbol{\phi}}_n^{\mathrm{T}}\boldsymbol{\Phi}_{\mathrm{r}}^{\mathrm{T}}\mathbf{M}_{\mathrm{sb}} + \frac{1}{\tilde{\omega}_n^2}\mathbf{K}_{\mathrm{bs}}\boldsymbol{\Phi}_{\mathrm{r}}\tilde{\boldsymbol{\phi}}_n\tilde{\boldsymbol{\phi}}_n^{\mathrm{T}}\boldsymbol{\Phi}_{\mathrm{r}}^{\mathrm{T}}\mathbf{K}_{\mathrm{sb}}\end{aligned} \tag{A3}$$

We use (A1) and (A2) in (A3) to get, for $n = 1, \ldots, N_{\mathrm{r}}$,

$$\tilde{\mathbf{S}}_n = \omega_n^2\mathbf{M}_{\mathrm{bs}}\boldsymbol{\phi}_n\boldsymbol{\phi}_n^{\mathrm{T}}\mathbf{M}_{\mathrm{sb}} - \mathbf{M}_{\mathrm{bs}}\boldsymbol{\phi}_n\boldsymbol{\phi}_n^{\mathrm{T}}\mathbf{K}_{\mathrm{sb}} - \mathbf{K}_{\mathrm{bs}}\boldsymbol{\phi}_n\boldsymbol{\phi}_n^{\mathrm{T}}\mathbf{M}_{\mathrm{sb}} + \frac{1}{\omega_n^2}\mathbf{K}_{\mathrm{bs}}\boldsymbol{\phi}_n\boldsymbol{\phi}_n^{\mathrm{T}}\mathbf{K}_{\mathrm{sb}} \tag{A4}$$

But this is exactly expression (34) for $\mathbf{S}_n$. Hence $\tilde{\mathbf{S}}_n = \mathbf{S}_n$ for $n = 1, \ldots, N_{\mathrm{r}}$. In other words, the original and reduced subsystems share the same first N_{r} coupling matrices.

ACKNOWLEDGEMENTS

This work is partly supported by the U.S.–Israel Binational Science Foundation (BSF) fund (Grant No. 97-00120), and by the Fund for the Promotion of Research at the Technion. The first author would like to thank Peter Pinsky, Charles Steele and Bob Taylor for useful discussions.

REFERENCES

1. Friswell MI. Candidate reduced order models for structural parameter estimation. *Journal of Vibration and Acoustics* (ASME) 1990; **112**:93–97.
2. Chiprout E, Nguyen T. Survey of model reduction techniques for analysis of package and interconnect models of high-speed designs. In *Proceedings of the 6th IEEE Meeting on Electrical Performance of Electronic Packaging*, IEEE, Piscataway, NJ, 1997; 251–254.

3. Mukherjee T, Fedder GK, Ramaswamy D, White J. Emerging simulation approaches for micromachined devices. *IEEE Transactions on Computer-Aided Design of Integrated Circuits and Systems* 2000; **19**: 1572–1589.
4. Cangellaris AC, Zhao L. Model order reduction techniques for electromagnetic macromodelling based on finite methods. *International Journal for Numerical Modelling Electronic Networks Devices Fields* 2000; **13**:181–197.
5. Livne E, Blando GD. Reduced-order design-oriented stress analysis using combined direct and adjoint solutions. *AIAA Journal* 2000; **38**:898–909.
6. Morari M, Zafiriou E. *Robust Process Control*. Prentice-Hall: Englewood Cliffs, NJ, 1989.
7. Meirovitch L. *Computational Methods in Structural Dynamics*. Sijthoff & Noordhoff, Alphen aan den Rijn: The Netherlands, 1980.
8. Moore BC. Principal component analysis in linear systems: controllability, observability and model reduction. *IEEE Transactions on Automatic Control* 1981; **26**:17–32.
9. Bisplinghoff RL, Ashley H. *Principles of Aeroelasticity*. Dover: New York, 1975.
10. Craig RR. Substructure methods in vibration. *Journal of Vibration and Acoustics* (ASME) 1995; **117**: 207–213.
11. Hyland DC, Bernstein DS. The optimal projection equations and the relationships among the methods of Wilson, Skelton and Moore. *IEEE Transactions on Automatic Control* 1985; **30**:1201–1211.
12. Patlashenko I, Givoli D, Barbone PE. Time-stepping schemes for systems of Volterra integro-differential equations. *Computer Methods in Applied Mechanics and Engineering* 2001; **190**:5691–5718.
13. Barbone P, Givoli D, Patlashenko I. Optimal modal reduction of vibrating substructures. *International Journal for Numerical Methods in Engineering* 2003; **57**:341–369.
14. Steele CR. Shells with edge loads of rapid variation—II. *Journal of Applied Mechanics* (ASME) 1965; **32**:87–98.
15. Keller JB, Givoli D. Exact non-reflecting boundary conditions. *Journal of Computational Physics* 1989; **82**:172–192.
16. Givoli D, Keller JB. A finite element method for large domains. *Computer Methods in Applied Mechanics and Engineering* 1989; **76**:41–66.
17. Givoli D, Rivkin L, Keller JB. A finite element method for domains with corners. *International Journal for Numerical Methods in Engineering* 1992; **35**:1329–1345.
18. Goldman D, Barbone PE. 'Dirichlet to Neumann maps for the representation of equipment with weak nonlinearities. In *Proceedings of the 1996 ASME Winter Annual Meeting*, vol. 22, Atlanta, GA, USA, November 96, ASME Noise Control and Acoustics Division, New York, NY, 1996; 71–76.
19. Cherukuri A, Barbone PE. High modal density approximations for equipment in the time domain. *Journal of the Acoustical Society of America* 1998; **104**:2048–2053.
20. Barbone PE, Cherukuri A, Goldman D. Canonical representations of complex vibratory subsystems: time domain Dirichlet to Neumann maps. *International Journal of Solids and Structures* 2000; **37**:2825–2857.
21. Givoli D. Exact representations on artificial interfaces and applications in mechanics. *Applied Mechanics Reviews* 1999; **52**:333–349.
22. Trefethen LN, Bau D III. *Numerical Linear Algebra*. SIAM: Philadelphia, 1997.
23. Hughes TJR. *The Finite Element Method*. Prentice-Hall: Englewood Cliffs, NJ, 1987.

